Hindawi Publishing Corporation
Physics Research International
Volume 2014, Article ID 619360, 10 pages
http://dx.doi.org/10.1155/2014/619360

Research Article

How Much Asymmetry of Colliding Pair Affects Nuclear Dynamics at Balance Point?

Supriya Goyal

Department of Physics, GSSDGS Khalsa College, Patiala 147001, India

Correspondence should be addressed to Supriya Goyal; ashuphysics@gmail.com

Received 5 May 2014; Accepted 21 July 2014; Published 20 August 2014

Academic Editor: Rajeev K. Puri

Using the quantum molecular dynamics model, we study the nuclear dynamics at the balance energy of mass asymmetric colliding nuclei by keeping the total mass of the system fixed and by varying the mass asymmetry ($\eta = (A_T - A_P)/(A_T + A_P)$, where A_T and A_P are the masses of the target and projectile, resp.) of the reaction. In particular, we study the various quantities like average and maximum density and temperature, collision rate, participant-spectator matter, anisotropic ratio, relative momentum, and their mass asymmetry and mass dependence. Our results indicate sizeable effect of mass asymmetry on these quantities.

1. Introduction

It is now well established that collective transverse flow of the nucleons is a signature of the interaction and can provide information about the equation of state (EoS) as well as nucleon-nucleon (nn) cross-section of the nuclear matter. Extensive studies have been done over the past three decades on the sensitivity of collective transverse flow towards the nuclear EoS, nn cross-section, and entrance channel parameters such as incident energy of projectile, size of the system ($A_{\mathrm{TOT}} = A_T + A_P$), and colliding geometry (i.e., impact parameter) [1–9]. The disappearance of flow is predicted to appear at some incident energy, which is termed as balance energy (E_{bal}) [10]. This balance energy has been subjected to extensive theoretical and experimental calculations to know its accurate value as well as its mass and impact parameter dependence [11–22].

Recently, the sensitivity of collective transverse flow and E_{bal} towards the mass asymmetry of the reaction has been carried out at different colliding geometries by keeping the total mass of the system fixed [20–22]. It has been found that almost independent of total system mass as well as colliding geometry, mass asymmetry has a uniform effect on the collective transverse flow and its disappearance [20]. This study was motivated from the recent observations by FOPI collaboration on the mass asymmetric reactions of ^{40}Ca + ^{197}Au and ^{197}Au + ^{40}Ca [23, 24]. They observe that flow in asymmetric reactions is a key observation for investigating the reaction dynamics. The difference between the reaction dynamics for symmetric and asymmetric reactions is attributed to the different role played by excitation energy in these reactions. In symmetric reactions most of the excitation energy is deposited in the form of compressional energy, whereas an asymmetric reaction deposits it in the form of thermal energy [25]. Therefore, in the present paper, this study is further extended for the central collisions to see the effect of mass asymmetry of the reaction on the nuclear dynamics at the balance energy. Similar work has been carried out by Sood and Puri [26] for the nearly symmetric and symmetric reactions at the balance energy, but the role of mass asymmetry in the participant-spectator matter, average and maximum density and temperature, net collisions, anisotropic ratio, relative momentum, and the mass dependence of these quantities is not taken care of. This has been taken care of in the present study. The study is made within the framework of quantum molecular dynamics (QMD) model [12–18, 20–22, 25–44], which is explained in Section 2. Results and discussion are explained in Section 3 and finally we summarize the results in Section 4.

2. The Model

The quantum molecular dynamics model [12–18, 20–22, 25–44] simulates the reaction on an event by event basis. Here each nucleon i is represented by a Gaussian wave packet with a width of $\sqrt{L}$ centered around the mean position $\vec{r}_i(t)$ and mean momentum $\vec{p}_i(t)$. Here each nucleon is represented by a coherent state of the form

$$\phi_i(\vec{r},\vec{p},t) = \frac{1}{(2\pi L)^{3/4}} e^{[-\{\vec{r}-\vec{r}_i(t)\}^2/4L]} e^{[i\vec{p}_i(t)\cdot\vec{r}/\hbar]}. \quad (1)$$

The Wigner distribution of a system with $A_T + A_P$ nucleons is given by

$$f(\vec{r},\vec{p},t) = \sum_{i=1}^{A_T+A_P} \frac{1}{(\pi\hbar)^3} e^{[-\{\vec{r}-\vec{r}_i(t)\}^2/2L]} e^{[-\{\vec{p}-\vec{p}_i(t)\}^2 2L/\hbar^2]}, \quad (2)$$

with $L = 1.08\,\text{fm}^2$.

The center of each Gaussian (in the coordinate and momentum space) is chosen by the Monte Carlo procedure. The momentum of nucleons (in each nucleus) is chosen between zero and local Fermi momentum [$= \sqrt{2m_i V_i(\vec{r})}$; $V_i(\vec{r})$ is the potential energy of nucleon i]. Naturally, one has to take care that the nuclei, thus generated, have right binding energy and proper root mean square radii.

The centroid of each wave packet is propagated using the classical equations of motion:

$$\frac{d\vec{r}_i}{dt} = \frac{dH}{d\vec{p}_i}, \qquad \frac{d\vec{p}_i}{dt} = -\frac{dH}{d\vec{r}_i}, \quad (3)$$

where the Hamiltonian is given by

$$H = \sum_i \frac{\vec{p}_i^{\,2}}{2m_i} + V^{\text{tot}}. \quad (4)$$

Our total interaction potential V^{tot} reads as

$$V^{\text{tot}} = V^{\text{Loc}} + V^{\text{Yuk}} + V^{\text{Coul}} + V^{\text{MDI}} \quad (5)$$

with

$$V^{\text{Loc}} = t_1\delta(\vec{r}_i - \vec{r}_j) + t_2\delta(\vec{r}_i - \vec{r}_j)\,\delta(\vec{r}_i - \vec{r}_k), \qquad V^{\text{Yuk}} = \frac{t_3 e^{-|\vec{r}_i-\vec{r}_j|/\mu}}{\left(\left|\vec{r}_i - \vec{r}_j\right|\mu\right)}, \quad (6)$$

with $\mu = 1.5$ fm and $t_3 = -6.66$ MeV.

The static (local) Skyrme interaction can further be parameterized as

$$V^{\text{Loc}} = \alpha\left(\frac{\rho}{\rho_o}\right) + \beta\left(\frac{\rho}{\rho_o}\right)^{\gamma}. \quad (7)$$

Here α, β, and γ are the parameters that define equation of state. The momentum-dependent interaction is obtained by parameterizing the momentum dependence of the real part of the optical potential. The final form of the potential reads as

$$V^{\text{MDI}} \approx t_4 \ln^2\left[t_5\left(\vec{p}_i - \vec{p}_j\right)^2 + 1\right]\delta\left(\vec{r}_i - \vec{r}_j\right). \quad (8)$$

Here $t_4 = 1.57$ MeV and $t_5 = 5\times10^{-4}$ MeV^{-2}. A parameterized form of the local plus momentum-dependent interaction (MDI) potential (at zero temperature) is given by

$$V = \alpha\left(\frac{\rho}{\rho_0}\right) + \beta\left(\frac{\rho}{\rho_0}\right)^{\gamma} + \frac{\delta\ln^2\left[\epsilon(\rho/\rho_0)^{2/3} + 1\right]\rho}{\rho_0}. \quad (9)$$

The parameters α, β, and γ in above equation must be readjusted in the presence of momentum-dependent interactions so as to reproduce the ground state properties of the nuclear matter. The set of parameters corresponding to different equations of state can be found in [37].

3. Results and Discussion

For the present analysis, we simulated the reactions of ${}^{17}_{8}\text{O} + {}^{23}_{11}\text{Na}$ ($\eta = 0.15$), ${}^{14}_{7}\text{N} + {}^{26}_{12}\text{Mg}$ ($\eta = 0.3$), ${}^{10}_{5}\text{B} + {}^{30}_{14}\text{Si}$ ($\eta = 0.5$), and ${}^{6}_{3}\text{Li} + {}^{34}_{16}\text{S}$ ($\eta = 0.7$) for $A_{\text{TOT}} = 40$, ${}^{36}_{18}\text{Ar} + {}^{44}_{20}\text{Ca}$ ($\eta = 0.1$), ${}^{28}_{14}\text{Si} + {}^{52}_{24}\text{Cr}$ ($\eta = 0.3$), ${}^{20}_{10}\text{Ne} + {}^{60}_{28}\text{Ni}$ ($\eta = 0.5$), and ${}^{10}_{5}\text{B} + {}^{70}_{32}\text{Ge}$ ($\eta = 0.7$) for $A_{\text{TOT}} = 80$, ${}^{70}_{32}\text{Ge} + {}^{90}_{40}\text{Zr}$ ($\eta = 0.125$), ${}^{54}_{26}\text{Fe} + {}^{106}_{48}\text{Cd}$ ($\eta = 0.325$), ${}^{40}_{20}\text{Ca} + {}^{120}_{52}\text{Te}$ ($\eta = 0.5$), and ${}^{24}_{12}\text{Mg} + {}^{136}_{58}\text{Ce}$ ($\eta = 0.7$) for $A_{\text{TOT}} = 160$, and ${}^{108}_{48}\text{Cd} + {}^{132}_{56}\text{Ba}$ ($\eta = 0.1$), ${}^{84}_{38}\text{Sr} + {}^{156}_{66}\text{Dy}$ ($\eta = 0.3$), ${}^{60}_{28}\text{Ni} + {}^{180}_{74}\text{W}$ ($\eta = 0.5$), and ${}^{36}_{18}\text{Ar} + {}^{204}_{82}\text{Pb}$ ($\eta = 0.7$) for $A_{\text{TOT}} = 240$, at their corresponding theoretical balance energies (taken from [20]). The balance energies at which these reactions are simulated were calculated using a momentum-dependent soft equation of state with standard energy-dependent cugnon cross-section and reduced impact parameter ($\hat{b} = b/b_{\max}$, where $b_{\max} = R_1 + R_2$; R_i is the radius of projectile or target) of 0.25. The values of parameters used in (9) for momentum-dependent soft equation of state are compressibility (K(MeV)) = 200, α(MeV) = −390, β(MeV) = 320, $\gamma = 1.14$, δ(MeV) = 1.57, and $\epsilon = 21.54$. The reactions are followed uniformly up to 500 fm/c.

In Figure 1, we display the $\langle\rho^{\text{avg}}\rangle/\rho_0$ (left column) and $\langle\rho^{\max}\rangle/\rho_0$ (right column) as a function of the reaction time. The values of $\langle\rho^{\text{avg}}\rangle$ and $\langle\rho^{\max}\rangle$ are calculated within a sphere of radius 2 fm around the center of mass. The density is then computed at each time step during the reaction using

$$\rho(\vec{r},t) = \sum_{i=1}^{A_T+A_P} \frac{1}{(2\pi L)^{3/2}} e^{(-(\vec{r}-\vec{r}_i(t))^2/2L)}. \quad (10)$$

The results are displayed by varying η from 0.1 to 0.7 for different mass ranges; that is, $A_{\text{TOT}} = 40$, 80, 160, and 240. It is clear from the figure that the maximal value of $\langle\rho^{\text{avg}}\rangle/\rho_0$ decreases with increase in η. A similar trend can be seen for the evolution of $\langle\rho^{\max}\rangle/\rho_0$ at all mass ranges. This is due to the decrease in the interaction region with increase in mass asymmetry of the reaction. Further, one should note that

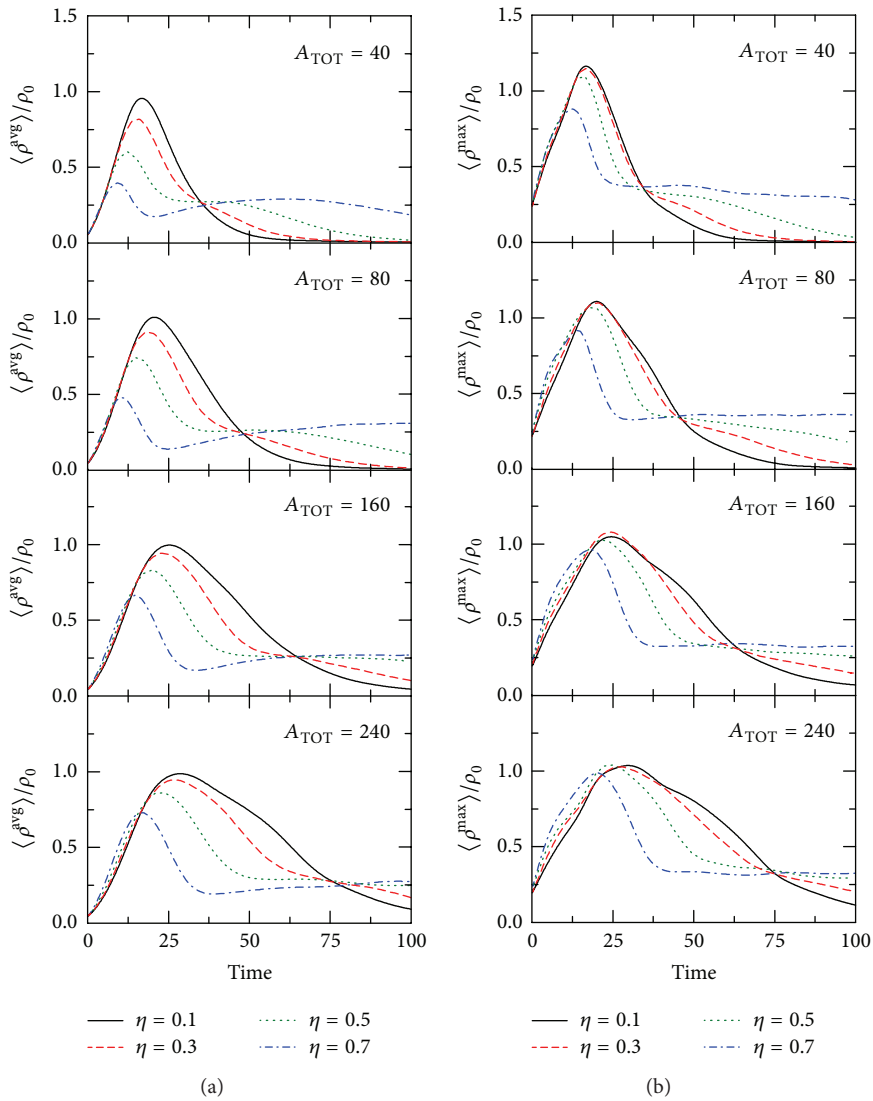

FIGURE 1: The time evolution of the average density $\langle\rho^{avg}\rangle/\rho_0$ (a) and maximum density $\langle\rho^{max}\rangle/\rho_0$ (b) reached in a central sphere of radius 2 fm for different system masses. The results for different asymmetries η = 0.1, 0.3, 0.5, and 0.7 are represented, respectively, by the solid, dashes, dotted, and dashed-dotted lines.

for nearly symmetric reactions with η = 0.1, the values of $\langle\rho^{avg}\rangle/\rho_0$ and $\langle\rho^{max}\rangle/\rho_0$ are comparable for the heavy systems, indicating the wide and uniform formation of dense matter in the central region of 2 fm radius. This is similar to what predicted in [26]. However, a nonhomogeneous nature of the dense matter is seen for lighter systems at all asymmetries. For each mass range, as η increases and for each η, as A_{TOT} decreases, the incident energy increases. Therefore, for each A_{TOT}, the reactions with larger asymmetries and for each η, the systems with smaller A_{TOT}, finishes much earlier. Similarly, the peak values of the densities are also delayed for reactions of heavy colliding nuclei and smaller asymmetries. Also, one should note that the time of saturation increases with increase in η.

Similar to Figure 1, we display the net collision rate as a function of the reaction time in Figure 2. It is directly connected with the density. Due to the decrease in interaction volume with increase in mass asymmetry of colliding nuclei, the net collision rate decreases with increase in η and the interactions among nucleons also cease earlier. This is observed for all system mass ranges. As expected, with increase in system mass, opposite trend is observed for each η. This behavior is also evident from the density profile (see Figure 1).

It is well known that balance energy represents a counterbalancing between the attractive and repulsive forces; therefore, this fact should also be reflected in quantities like spectator and participant matter. In Figure 3, we display the normalized spectator (a, b) and participant (c, d) matter as a function of reaction time. The results are displayed for different asymmetries by keeping the total mass of the system fixed as A_{TOT} = 80 and 240. All nucleons having experienced at least one collision are termed as participant and the remaining matter is termed as spectator matter. One

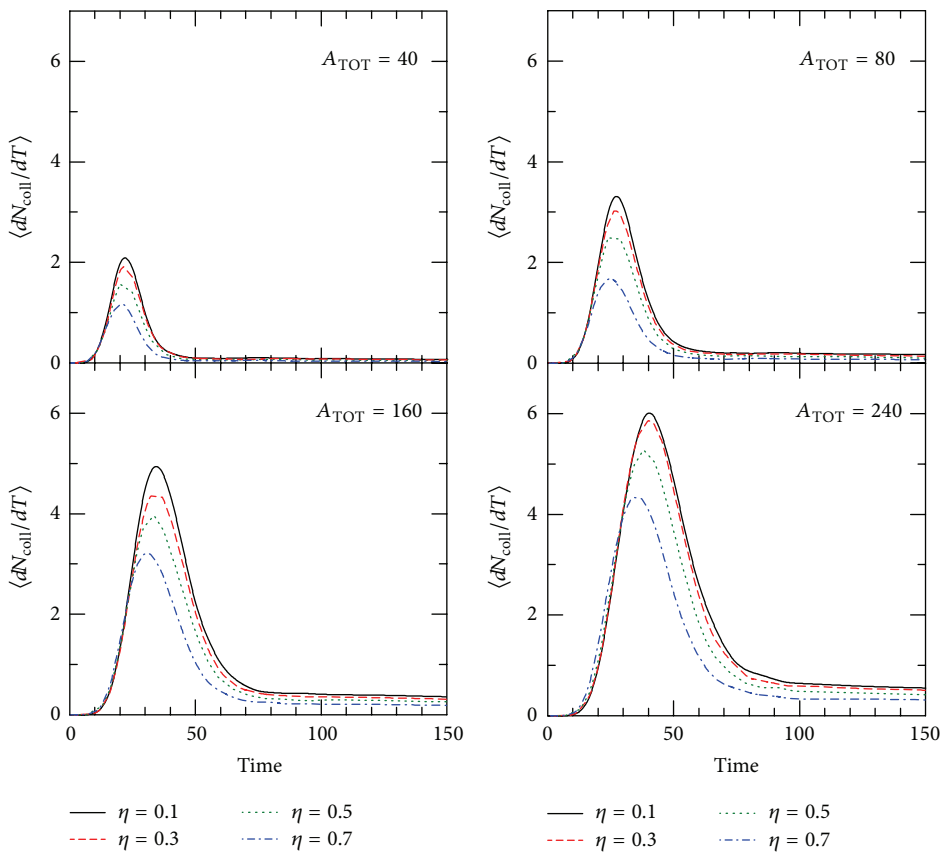

Figure 2: Same as Figure 1, but for the rate of allowed collisions versus reaction time.

can also define spectator and participant matter in terms of rapidity distribution; however, the results are similar for both definitions, as shown in [26]. From the figure, one clearly sees that at the start of the reaction, all nucleons constitute spectator matter; therefore, no participant matter exists at initial time (i.e., $t = 0$ fm/c). Due to decrease in the number of nn collisions with increase in η, the spectator (participant) matter increases (decreases) with increase in η. Similar behavior is seen for different system masses.

In Figure 4, we display the time evolution of relative momentum $\langle K_R \rangle$ (a) and anisotropy ratio $\langle R_a \rangle$ (b) for different η and A_{TOT}. The anisotropy ratio $\langle R_a \rangle$ is defined as [38–44]

$$\langle R_a \rangle = \frac{\sqrt{\langle p_x^2 \rangle} + \sqrt{\langle p_y^2 \rangle}}{2\sqrt{\langle p_z^2 \rangle}}. \tag{11}$$

This anisotropy ratio $\langle R_a \rangle$ is an indicator of the global equilibrium of the system as it does not depend on the local density. The full global equilibrium averaged over large number of events will correspond to $\langle R_a \rangle = 1$. The second quantity, the relative momentum $\langle K_R \rangle$ of two colliding spheres, is defined as [38–44]

$$\langle K_R \rangle = \left\langle \frac{\left|\vec{P}_P(\vec{r},t) - \vec{P}_T(\vec{r},t)\right|}{\hbar} \right\rangle, \tag{12}$$

where

$$\vec{P}_i(\vec{r},t) = \frac{\sum_{j=1}^{A} \vec{P}_j(t)\,\rho_j(\vec{r},t)}{\rho_j(\vec{r},t)}, \quad i = 1, 2. \tag{13}$$

Here $\vec{P}_j$ and ρ_j are the momentum and density experienced by the jth particle and i stands either for target or projectile. As noted, this quantity measures deviation from a single Fermi sphere and hence represents local equilibrium. Such a concept of local equilibrium is commonly used in the hydrodynamical model. Obviously, with the passage of the time, density in a central sphere will decrease due to lesser and lesser nucleons and, as a result, $\langle K_R \rangle$ will also decrease. On the other hand, no such density dependence exists for $\langle R_a \rangle$. The anisotropy ratio $\langle R_a \rangle$ will saturate after the finishing of the reaction. From the figure, we see that $\langle K_R \rangle$ decreases as the reaction proceeds, while $\langle R_a \rangle$ ratio increases and saturates after the high dense phase is over. Due to increase in incident energy with η, thermalization is little bit better achieved for larger η. Similar behavior is observed for each fixed system mass. However, for each η, due to high density obtained in heavier systems, the thermalization is better achieved compared to lighter colliding nuclei.

Temperature is one of the associated quantities linked with a dense matter. In principle, one can define true temperature only for a thermalized and equilibrated matter. Since in heavy-ion collisions the matter is nonequilibrated,

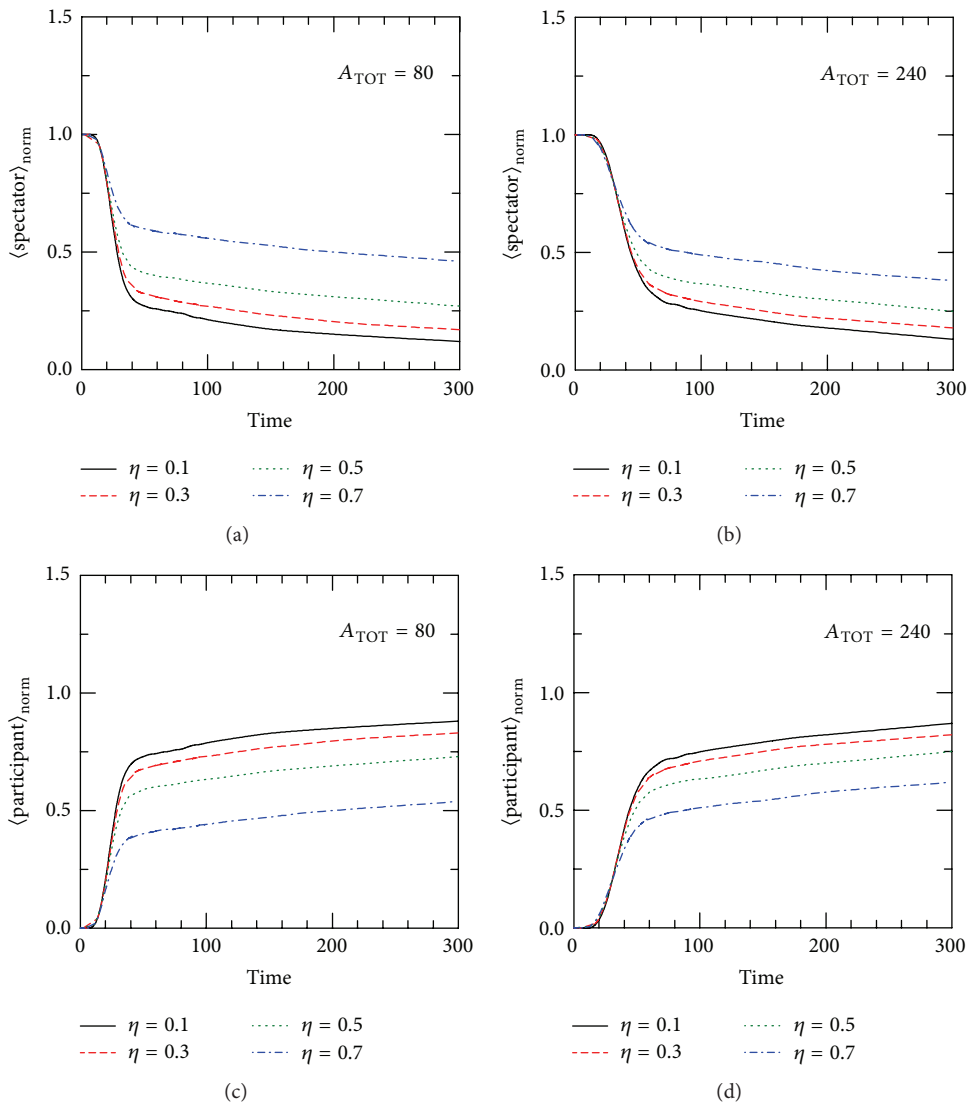

FIGURE 3: The time evolution of the normalized spectator matter (a, b) and participant matter (c, d). The results for total system mass A_{TOT} = 80 and 240 are displayed in left and right columns. Lines have the same meaning as in Figure 1.

one cannot talk of temperature. One can only look in terms of the local environment. In our case, we follow the description of the temperature as given in [45–47]. The extraction of the temperature T is based on the local density approximation; that is, one deduces the temperature in a volume element surrounding the position of each particle at a given time step [45–47]. In present case each local volume element of nuclear matter in coordinate space and time has some temperature defined by the diffused edge of the deformed Fermi distribution consisting of two colliding Fermi spheres, which is typical for a nonequilibrium momentum distribution in heavy-ion collisions. In this formalism which is dubbed the hot Thomas-Fermi approach [45–47], one determines extensive quantities such as the density and kinetic energy as well as entropy with the help of momentum distributions at a given temperature. Using this formalism, we also extracted the average and maximum temperature within a central sphere of 2 fm radius as described in the case of density.

In Figure 5, we display the mass dependence of the maximal values of $\langle T^{avg}\rangle$, $\langle T^{max}\rangle$, $\langle \rho^{avg}\rangle$, and $\langle \rho^{max}\rangle$ as well as the final stage value of (allowed) nn collisions and spectator/participant matter. For the nearly symmetric reaction having $\eta = 0.1$, the dependence is similar to that shown in [26]. All the quantities follow a power law behavior $\propto A_{TOT}^{\tau}$. The values of power factor τ are displayed in the figure. It shows that the dependence of temperature reached in the central region is in sharp contradiction to the evolution of density reached in the central region because the dependence of maximal value of $\langle \rho^{avg}\rangle$ and $\langle \rho^{max}\rangle$ is very weak on system mass for all η while weak dependence on system mass is seen in case of temperature. This is due to the fact that the temperature depends also on the kinetic energy

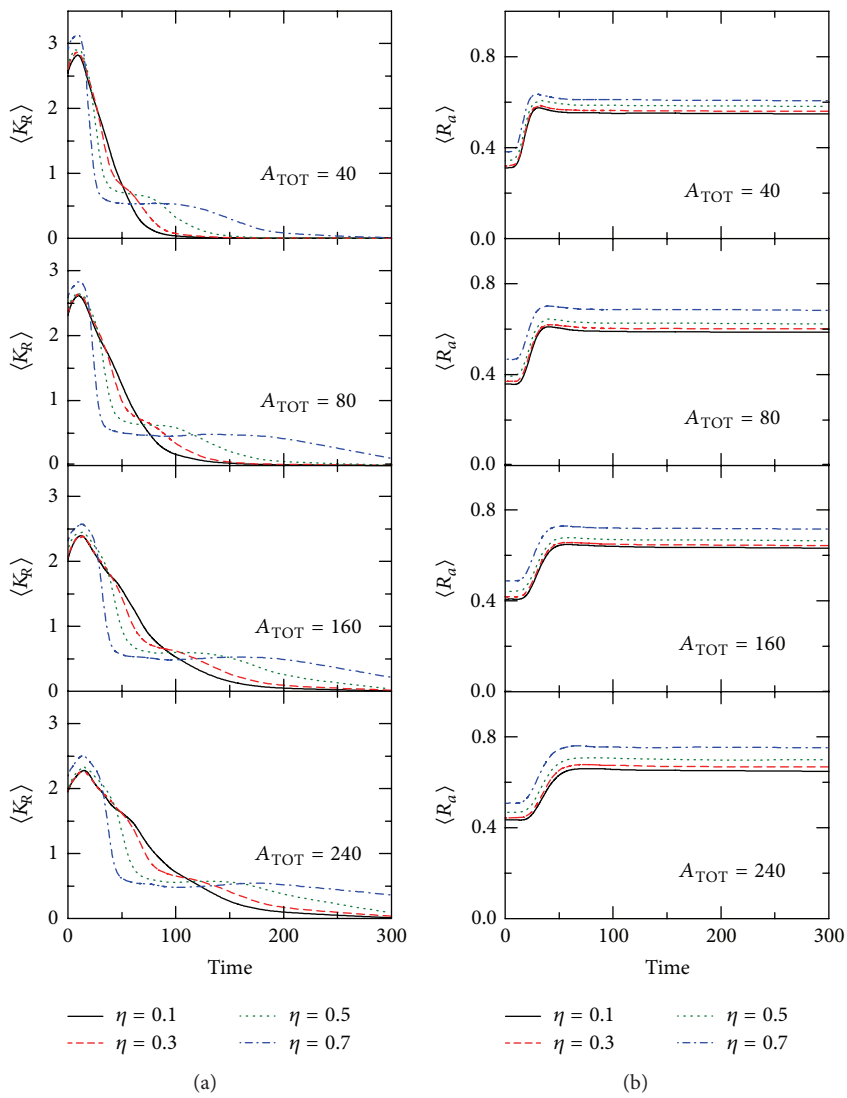

Figure 4: Same as Figure 1, but for the relative momentum $\langle K_R \rangle$ (a) and anisotropy ratio $\langle R_a \rangle$ (b).

(i.e., excitation energy) of the system [45–47]. For a given colliding geometry, the maximal value of $\langle T^{avg} \rangle$ and $\langle T^{max} \rangle$ also depends on the bombarding energy rather than on the size of the interacting source [48]. Since, in our case, we have carried out the study at balance energy, which varies with the system mass, this in turn leads to dependence of temperature on the system mass due to the variation in the bombarding energy. At a fixed bombarding energy, dependence could be different. For nn collisions, one sees a linear enhancement with the system mass for each η. Naturally, at a fixed energy, the nn collisions should scale as A_{TOT} [26] and it is seen for each η. The spectator and participant matter are nearly independent of the mass of the system for each η.

In Figure 6, we display the mass asymmetry dependence of the maximal values of $\langle T^{avg} \rangle$, $\langle T^{max} \rangle$, $\langle \rho^{avg} \rangle$, and $\langle \rho^{max} \rangle$ as well as the final stage value of (allowed) nn collisions and spectator/participant matter. The results are displayed for different mass ranges. Lines are the linear fits ($\propto m\eta$). We find a clear dependence of quantities on η. The dependence of maximal value of $\langle \rho^{avg} \rangle$ and $\langle \rho^{max} \rangle$ on η decreases with increase in system mass while in case of $\langle T^{avg} \rangle_{max}$ and $\langle T^{max} \rangle_{max}$; different trend is seen which is due to the same reason as explained in earlier paragraph, while for nn collisions an opposite trend is observed. The nn collisions also decrease with increase in η, but due to larger interaction volume in heavier systems, heavier colliding nuclei show large η dependence. Obviously, the spectator matter and the participant matter will behave oppositely. For each system mass, the spectator (participant) matter increases (decreases) with increase in η and similar to density; the η dependence decreases with increase in total mass of the system. From this figure, it is clear that mass asymmetry of the reaction has a significant role in the nuclear dynamics of the reaction. Therefore, while studying various phenomenon in the intermediate energy heavy-ion collisions, one should take care of the mass asymmetry of the reaction.

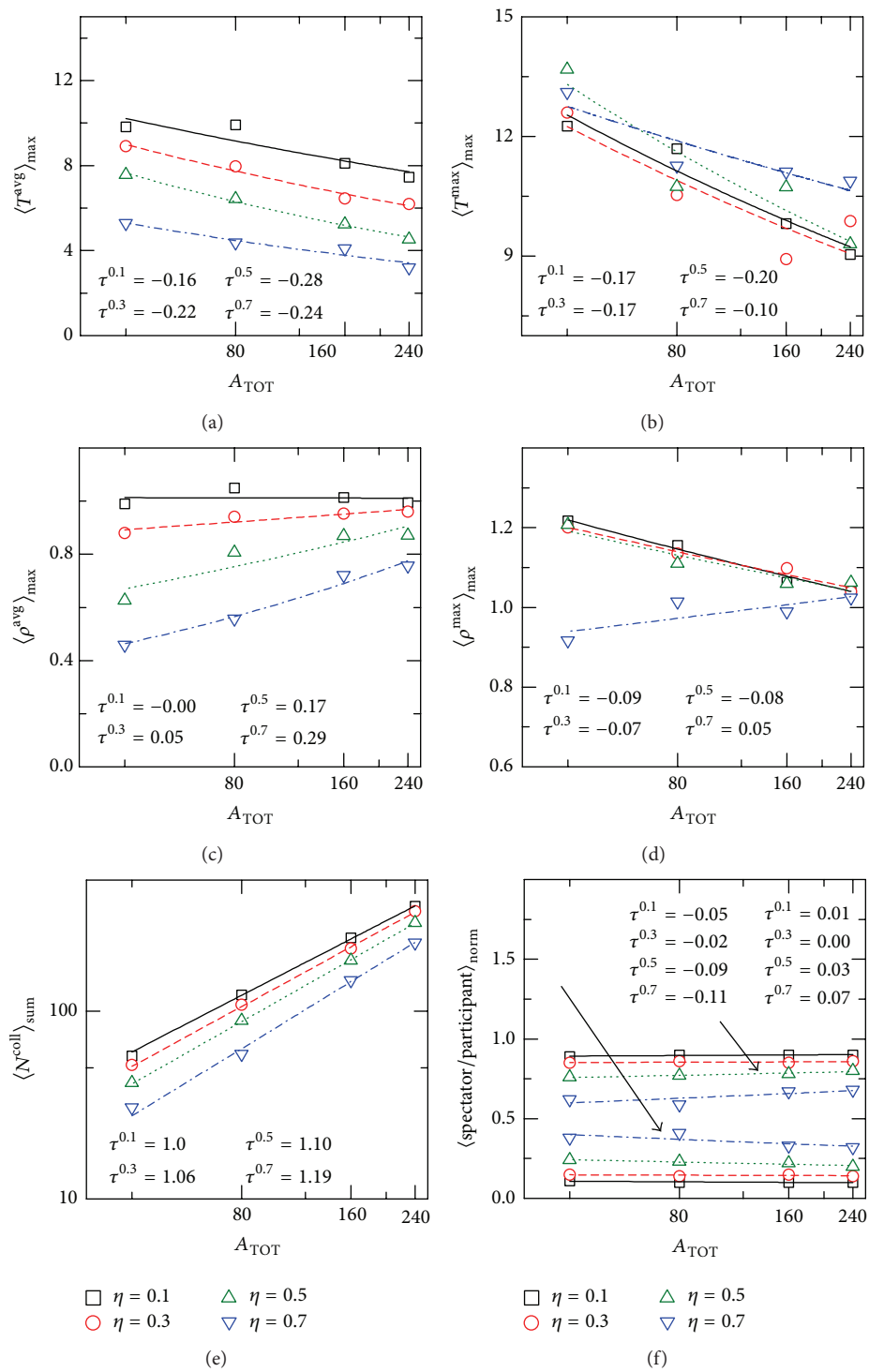

FIGURE 5: The maximal value of the average temperature $\langle T^{avg}\rangle_{max}$ (a), maximum temperature $\langle T^{max}\rangle_{max}$ (b), average density $\langle \rho^{avg}\rangle_{max}$ (c), maximum density $\langle \rho^{max}\rangle_{max}$ (d), total number of the allowed collisions obtained at the final stage (e), and final saturated spectator/participant matter (f) as a function of total mass of the system. The results for different asymmetries $\eta = 0.1$, 0.3, 0.5, and 0.7 are represented, respectively, by the open squares, circles, triangles, and inverted triangles. The lines are power law ($\propto A_{TOT}^{\tau}$) fits to the calculated results. The values of the power factor τ are displayed in the figure for various quantities.

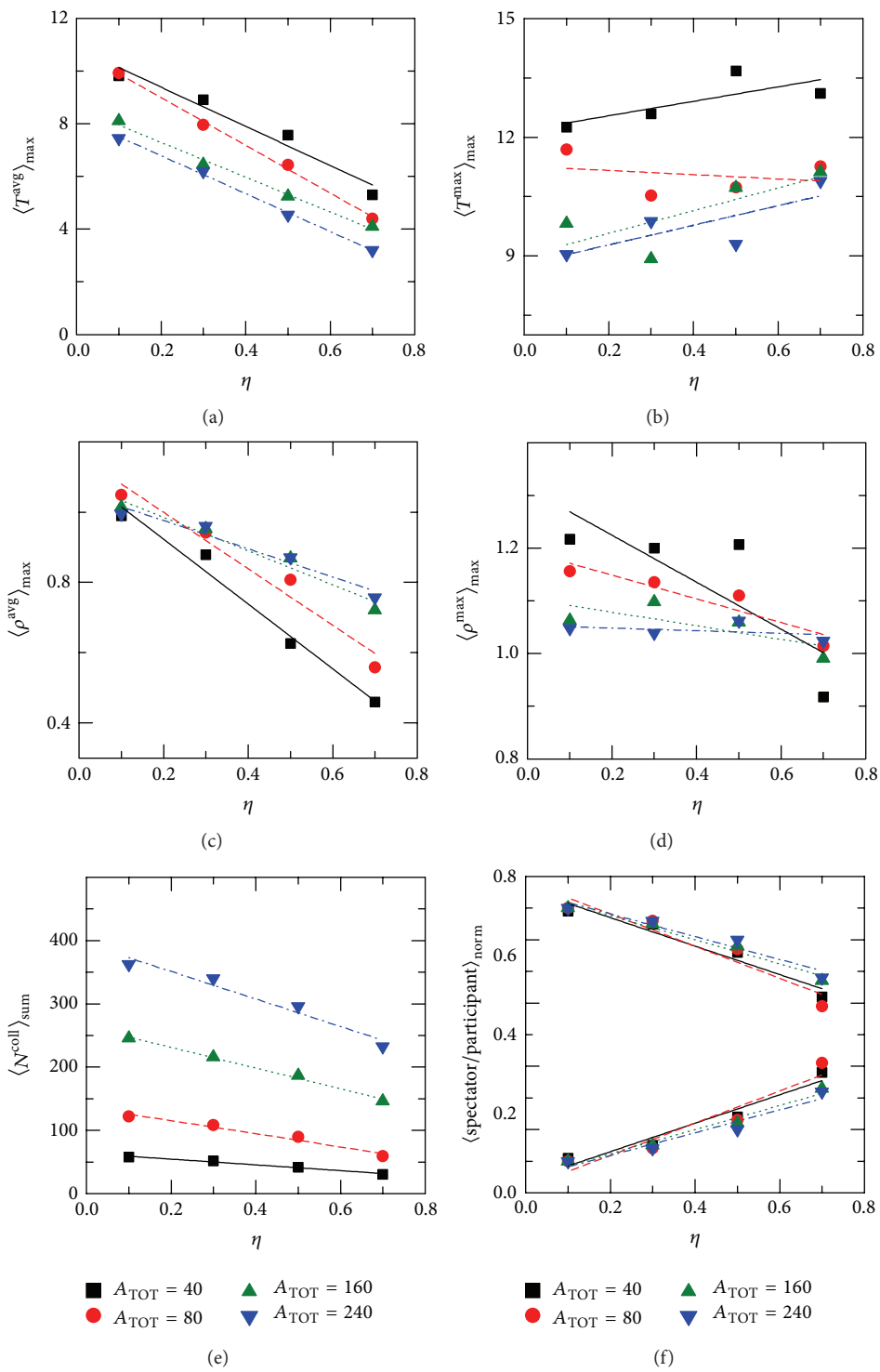

FIGURE 6: Same as Figure 5, but as a function of mass asymmetry of the reaction. The results for different system masses A_{TOT} = 40, 80, 160, and 240 are represented, respectively, by the solid squares, circles, triangles, and inverted triangles. Lines are the linear fits ($\propto m\eta$).

4. Summary

We studied the nuclear dynamics (particularly, average and maximum temperature and density, collision rate, participant-spectator matter, anisotropic ratio, relative momentum, and their mass asymmetry and mass dependence) at the balance energy of mass asymmetric reactions by keeping the total mass of the system fixed as 40, 80, 160, and 240 and varying the mass asymmetry of the reaction from 0.1 to 0.7. A sizeable effect of mass asymmetry on these quantities is

observed. Therefore one cannot ignore the presence of mass asymmetry of reaction while studying the various phenomena of intermediate energy heavy-ion reactions.

Conflict of Interests

The author declares that there is no conflict of interests regarding the publication of this paper.

References

[1] W. Scheid, H. Müller, and W. Greiner, "Nuclear shock waves in heavy-ion collisions," *Physical Review Letters*, vol. 32, pp. 741–745, 1974.

[2] H. A. Gustafsson, H. H. Gutbrod, B. Kolb et al., "Collective flow observed in relativistic nuclear collisions," *Physical Review Letters*, vol. 52, p. 1590, 1984.

[3] C. A. Ogilvie, D. A. Cebra, J. Clayton et al., "Transverse collective motion in intermediate-energy heavy-ion collisions," *Physical Review C*, vol. 40, article 2592, 1989.

[4] B. Bl, V. Koch, A. Lang, K. Weber, W. Cassing, and U. Mosel, "Origin of transverse momentum in relativistic heavy-ion collisions: microscopic study," *Physical Review C*, vol. 43, Article ID 2728, 1991.

[5] A. Andronic, W. Reisdorf, N. Herrmann et al., "Directed flow in Au+Au, Xe+CsI, and Ni+Ni collisions and the nuclear equation of state," *Physical Review C*, vol. 67, Article ID 034907, 2003.

[6] J. Łukasika, G. Augerb, M.L. Begemann-Blaich et al., "Directed and elliptic flow in ^{197}Au + ^{197}Au at intermediate energies," *Physics Letters B*, vol. 608, no. 3-4, pp. 223–230, 2005.

[7] Y. Zhang and Z. Li, "Elliptic flow and system size dependence of transition energies at intermediate energies," *Physical Review C*, vol. 74, Article ID 014602, 2006.

[8] B. Hong, Y. J. Kim, D. H. Kang et al., "Proton and deuteron rapidity distributions and nuclear stopping in ^{96}Ru(^{96}Zr) + ^{96}Ru(^{96}Zr) collisions at 400*A*MeV," *Physical Review C*, vol. 66, Article ID 034901, 2002.

[9] J. Lukasik and W. Trautmann, "Collective flow in heavy ion collisions at intermediate energies," in *Proceedings of the 23rd International Nuclear Physics Conference (INPC '07)*, vol. 2, p. 513, 2007.

[10] D. Krofcheck, W. Bauer, G. M. Crawley et al., "Disappearance of flow in heavy-ion collisions," *Physical Review Letters*, vol. 63, p. 2028, 1989.

[11] D. J. Magestro, W. Bauer, O. Bjarki et al., "Disappearance of transverse flow in Au+Au collisions," *Physical Review C*, vol. 61, no. 2, Article ID 021602(R), 2000.

[12] S. Kumar, M. K. Sharma, R. K. Puri, K. P. Singh, and I. M. Govil, "Impact parameter dependence of the disappearance of flow and in-medium nucleon-nucleon cross section," *Physical Review C*, vol. 58, no. 6, pp. 3494–3499, 1998.

[13] A. D. Sood and R. K. Puri, "Study of balance energy in central collisions for heavier nuclei," *Physics Letters B*, vol. 594, no. 3-4, pp. 260–264, 2004.

[14] A. D. Sood and R. K. Puri, "Mass dependence of disappearance of transverse in-plane flow," *Physical Review C—Nuclear Physics*, vol. 69, no. 5, Article ID 054612, 2004.

[15] A. D. Sood and R. K. Puri, "Influence of momentum-dependent interactions on balance energy and mass dependence," *The European Physical Journal A: Hadrons and Nuclei*, vol. 30, no. 3, pp. 571–577, 2006.

[16] A. D. Sood and R. K. Puri, "Systematic study of the energy of vanishing flow: role of equations of state and cross sections," *Physical Review C*, vol. 73, Article ID 067602, 2006.

[17] A. D. Sood and R. K. Puri, "Participant-spectator matter at the energy of vanishing flow," *Physical Review C*, vol. 79, Article ID 064618, 2009.

[18] R. Chugh and R. K. Puri, "Importance of momentum dependent interactions at the energy of vanishing flow," *Physical Review C*, vol. 82, Article ID 014603, 2010.

[19] D. J. Magestro, W. Bauer, and G. D. Westfall, "Isolation of the nuclear compressibility with the balance energy," *Physical Review C*, vol. 62, no. 4, pp. 416031–416034, 2000.

[20] S. Goyal and R. K. Puri, "On the sensitivity of the energy of vanishing flow towards mass asymmetry of colliding nuclei," *Nuclear Physics A*, vol. 853, no. 1, pp. 164–172, 2011.

[21] S. Goyal, "Role of the mass asymmetry of reaction on the geometry of vanishing flow," *Nuclear Physics A*, vol. 856, pp. 154–161, 2011.

[22] S. Goyal, "Role of colliding geometry on the balance energy of mass-asymmetric systems," *Physical Review C*, vol. 83, Article ID 047604, 2011.

[23] O. Hartmann, *Untersuchung der niedrig-liegenden elektrischen Dipolstärke und der Zerfallsstruktur der semi-magischen Kerne 44 Ca und 140 Ce mittels elastischer Photonenstreuung und inelastischer Protonenstreuung [Dissertation]*, Technische Universität Darmstadt, 2003.

[24] K. J. Eskola, "Quark and gluon production in high energy nucleus-nucleus collisions," *Nuclear Physics B*, vol. 323, no. 1, pp. 37–52, 1989.

[25] J. Singh, *Clustering in heavy ion collisions: dynamical microscopic theory versus experiments [Ph.D. thesis]*, Panjab University, Chandigarh, India, 2001.

[26] A. D. Sood and R. K. Puri, "Nuclear dynamics at the balance energy," *Physical Review C*, vol. 70, Article ID 034611, 2004.

[27] E. Lehmann, R. K. Puri, A. Faessler, G. Batko, and S. W. Huang, "Consequences of a covariant description of heavy-ion reactions at intermediate energies," *Physical Review C*, vol. 51, p. 2113, 1995.

[28] R. K. Puri, C. Hartnack, and J. Aichelin, "Early fragment formation in heavy-ion collisions," *Physical Review C*, vol. 54, no. 1, pp. R28–R31, 1996.

[29] C. Hartnack, R. K. Puri, J. Aichelin et al., "Modelling the many-body dynamics of heavy ion collisions: present status and future perspective," *The European Physical Journal A*, vol. 1, pp. 151–169, 1998.

[30] R. K. Puri and J. Aichelin, "Simulated annealing clusterization algorithm for studying the multifragmentation," *Journal of Computational Physics*, vol. 162, no. 1, pp. 245–266, 2000.

[31] S. Kumar, S. Kumar, and R. K. Puri, "Medium mass fragment production due to momentum dependent interactions," *Physical Review C*, vol. 78, Article ID 064602, 2008.

[32] Y. K. Vermani and R. K. Puri, "Microscopic approach to the spectator matter fragmentation from 400 to 1000AMeV," *Europhysics Letters*, vol. 85, Article ID 62001, 5 pages, 2009.

[33] Y. K. Vermani and R. K. Puri, "Mass dependence of the onset of multifragmentation in low energy heavy-ion collisions," *Journal of Physics G: Nuclear and Particle Physics*, vol. 36, no. 10, Article ID 105103, 2009.

[34] Y. K. Vermani, J. K. Dhawan, S. Goyal, R. K. Puri, and J. Aichelin, "Study of fragmentation using clusterization algorithm with realistic binding energies," *Journal of Physics G: Nuclear and Particle Physics*, vol. 37, no. 1, Article ID 015105, 2010.

[35] S. Kumar, S. Kumar, and R. K. Puri, "Elliptical flow and isospin effects in heavy-ion collisions at intermediate energies," *Physical Review C*, vol. 81, Article ID 014611, 2010.

[36] S. Kumar, S. Kumar, and R. K. Puri, "Effect of the symmetry energy on nuclear stopping and its relation to the production of light charged fragments," *Physical Review C*, vol. 81, Article ID 014601, 2010.

[37] J. Aichelin, "'Quantum' molecular dynamics–a dynamical microscopic n-body approach to investigate fragment formation and the nuclear equation of state in heavy ion collisions," *Physics Reports*, vol. 202, pp. 233–360, 1991.

[38] J. K. Dhawan, *Multifragmentation in heavy-ion collisions: role of nuclear flow and momentum correlations [Ph.D. Thesis]*, Panjab University, Chandigarh, India, 2007.

[39] S. Gautam, R. Chugh, A. D. Sood, R. K. Puri, C. H. Hartnack, and J. Aichelin, "Isospin effects on the energy of vanishing flow in heavy-ion collisions," *Journal of Physics G: Nuclear and Particle Physics*, vol. 37, no. 8, Article ID 085102, 2010.

[40] S. Gautam, A. D. Sood, R. K. Puri, and J. Aichelin, "Isospin effects in the disappearance of flow as a function of colliding geometry," *Physical Review C*, vol. 83, Article ID 014603, 2011.

[41] S. Gautam, A. D. Sood, R. K. Puri, and J. Aichelin, "Sensitivity of the transverse flow to the symmetry energy," *Physical Review C*, vol. 83, Article ID 034606, 2011.

[42] S. Gautam, "Density and temperature of neutron-rich systems at the energy of vanishing flow in heavy-ion collisions," *Physical Review C*, vol. 83, Article ID 064604, 2011.

[43] S. Gautam and R. K. Puri, "Participant-spectator matter and thermalization of neutron-rich systems at the energy of vanishing flow," *Physical Review C*, vol. 85, Article ID 067601, 2012.

[44] S. Kaur and R. K. Puri, "Isospin effects on the energy of peak mass production," *Physical Review C*, vol. 87, Article ID 014620, 2013.

[45] D. T. Khoa, N. Ohtsuka, A. Faessler et al., "Microscopic study of thermal properties of the nuclear matter formed in heavy-ion collisions," *Nuclear Physics A*, vol. 542, no. 4, pp. 671–698, 1992.

[46] D. T. Khoa, N. Ohtsuka, M. A. Matin et al., "In-medium effects in the description of heavy-ion collisions with realistic NN interactions," *Nuclear Physics A*, vol. 548, pp. 102–130, 1992.

[47] R. K. Puri, N. Ohtsuka, E. Lehmann et al., "Temperature-dependent mean field and its effect on heavy-ion reactions," *Nuclear Physics A*, vol. 575, no. 4, pp. 733–765, 1994.

[48] R. K. Puri, E. Lehmann, A. Faessler, and S. W. Huang, "Study of non-equilibrium effects and thermal properties of heavy-ion collisions using a covariant approach," *Journal of Physics G*, vol. 20, no. 11, pp. 1817–1828, 1994.